THE JOURNAL OF PHYSICAL CHEMISTRY B

ARTICLE

pubs.acs.org/JPCB

Glass Formation and Thermodynamics of Supercooled Monatomic Liquids

Vo Van Hoang*

Department of Physics, Institute of Technology, National University of HochiMinh City, 268 Ly Thuong Kiet Street, District 10, HochiMinh City, Vietnam

Takashi Odagaki

Department of Physics, Tokyo Denki University, Hatoyama Hikigun, Saitama 350-0394 Japan

ABSTRACT: Atomic mechanism of glass formation of a supercooled simple monatomic liquid with Lennard-Jones−Gauss (LJG) interatomic potential is studied by molecular dynamics (MD) simulation. Supercooled and glassy states are obtained by cooling from the melt. Glassy state obtained at low temperatures is annealed for very long time, on the order of microsecond, and we find that glassy state remains unchanged and that the long-lived glassy state of a simple monatomic system in three dimensions is realized. We analyze the spatiotemporal properties of solid-like and liquid-like atoms that are defined by the Lindemann-like freezing criterion. The number of solid-like atoms, distributed throughout the liquid, increases with decreasing temperature toward glass transition and they form clusters. In the deeply supercooled region, almost all solid-like atoms form a single percolation cluster and its characteristic size increases sharply on further cooling. Glass formation in supercooled liquid occurs when a single percolation cluster of solid-like atoms involves a majority of atoms to form a relatively rigid solid phase. We also obtain several physical quantities of the system, including temperature dependence of mass density, Lindemann ratio, incoherent intermediate scattering function, α-relaxation time, evolution of radial distribution function, and local bond-pair orders detected by Honeycutt−Andersen analysis. We identify three characteristic temperatures related to the vitrification: a temperature at which crossover from liquid-like to solid-like dynamics occurs on cooling, the glass transition temperature, and the Vogel−Fulcher−Tammann temperature. Behavior of liquid-like atoms in glassy state has been analyzed and discussed.

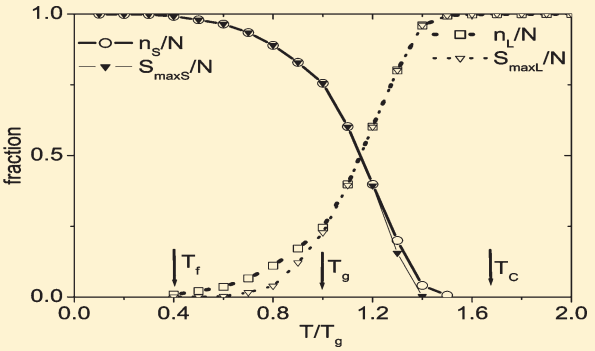

I. INTRODUCTION

Despite long and intensive efforts for decades, understanding of glass formation is far from complete, even for the simplest system, and it has been under intensive investigations by experiments, theoretical approaches, and computer simulations (see ref 1 and references therein). The difficulty lies in the fact that all glass formers are rather complex systems and both topological and chemical orders are hard to be decoupled. It is fairly desirable if one could succeed in producing a long-lived glassy state of a simple monatomic system, even in a computer, since one can study purely topological order in vitrification process and a theoretical framework for understanding the glass transition could be tested against it. In fact, many attempts have been made to create a single-component glass.[2−9] However, monatomic liquids can readily crystallize upon cooling from the melt or after just short annealing at low temperatures.[2−6] In order to avoid the crystallization of simple monatomic liquids, Dzugutov has proposed a pair potential.[10] This potential has an additional maximum in the Lennard-Jones (LJ) potential at a range typical of the next-nearest neighbor coordination distance in close-packed crystals, which suppresses the crystallization of the system. Although such potential can yield a glassy state, the glass was not long-lived and was transformed into a dodecagonal quasicrystal after long annealing.[11] Therefore, it is of interest if one can propose other simple pair interatomic potential that can yield a long-lived monatomic glass. It was found recently that a monatomic system with double-well interaction potential, i.e., the Lennard-Jones−Gauss (LJG) potential,[12] can produce a long-lived glass in three[13] and two dimensions.[14]

In this paper, we study the atomic mechanism of glass formation of a simple monatomic liquid with LJG interactomic potential in three dimensions. In the past, attention was paid only to the atoms involved in local icosahedral arrangement[15,16] or to the atoms of extremely low or high mobility[17] in order to highlight some features of a glass formation in supercooled liquids. It is difficult to clarify the atomic mechanism of glass formation just

Received: November 20, 2010
Revised: April 15, 2011

ACS Publications © XXXX American Chemical Society

by studying the clustering of the most immobile atoms or those involving in icosahedral order. On the other hand, the cooperative rearrangement of groups of atoms has long been thought to underlie the dramatic slowing down of liquid dynamics on cooling toward the glassy state, and there exists experimental evidence for cooperative rearranging regions (CRRs) on the nanometer length scale near the glass transition.[18−20] Taking these facts into account, we investigate the behavior of individual atoms in detail in the vitirification process. To this end, we classify atoms into two groups, solid-like and liquid-like, by a Lindemann-like freezing criterion[21,22] and investigate an atomic mechanism of glass formation by analyzing spatiotemporal properties of solid-like and liquid-like atoms. We also study the temperature dependence of thermodynamic and dynamic properties such as potential energy, mean squared displacement, diffusion constant, and local orders related to the glass formation. The crossover, glass transition, and Vogel−Fulcher temperatures are also determined.

The paper is organized as follows: In section II, we introduce the model system and explain the method for the MD simulation. Results are presented in sections III−V; in section III, we discuss about the stability of the glassy state and evolution of structure on cooling from the melt, thermodynamic and dynamical properties are presented in section IV, and in section V, atomic mechanism of glass transition is presented on the basis of spatiotemporal arrangement of solid-like and liquid-like atoms. Conclusions are given in the last section.

II. MODEL AND METHOD OF SIMULATION

We consider a system of single-component atoms that interact mutually through the LJG potential:[12,14]

$$V(r) = \varepsilon\left[\left(\frac{\sigma}{r}\right)^{12} - 2\left(\frac{\sigma}{r}\right)^{6}\right] - 1.5\varepsilon \exp\left[-\frac{(r-1.47\sigma)^2}{0.04\sigma^2}\right] \quad (1)$$

The LJG potential is a sum of the Lennard-Jones potential and a Gaussian contribution. Note that the LJG potential (eq 1) produces a long-lived glassy state in two[14] and three dimensions,[13] and thus we fixed the relative position, the relative depth, and the width of the Gaussian part so that glassy states can easily be formed. We performed the MD simulation in a cube containing 2744 atoms under periodic boundary conditions. We use the following LJ-reduced units in the present work: the length in unit of σ, temperature T in unit of ε/k_B, and time in unit of $\tau_0 = \sigma(m/\varepsilon)^{1/2}$. Here, k_B is the Boltzmann constant, σ is the atomic diameter, and m is the atomic mass. For Ar, we have $m = 0.66 \times 10^{-25}$ kg, ε/k_B = 118 K, σ = 3.84 Å, and therefore, $\tau_0 = \sigma(m/\varepsilon)^{1/2}$ = 2.44 ps. We used the Verlet algorithm and MD time step is $dt = 0.001\tau_0$ or 2.44 fs if taking Ar for testing. We employ *NPT* ensemble simulation where the temperature and pressure are controlled by the standard algorithm. The cutoff was applied to LJG potential at r = 2.5 (see refs 12−14). The initial simple cubic structure configuration was melted at constant zero pressure by relaxing the system for 2×10^5 MD steps at high temperature T_0 = 2.5. Then the system was cooled down from the melt at constant zero pressure. The temperature of the system was decreased linearly in time as $T = T_0 - \gamma n$ via simple atomic velocity rescaling. Here, $\gamma = 2 \times 10^{-6}$ per one MD step is the cooling rate (or 9.67×10^{10} K/s if taking Ar for testing), n is the number of MD steps, and T_0 = 2.5 is an initial temperature. In order to calculate the coordination number, bond-angle distributions, and

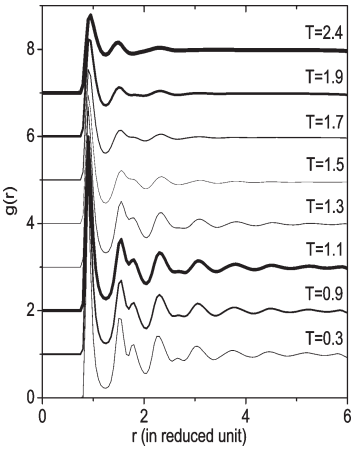

Figure 1. RDF at various temperatures, where RDF were calculated upon cooling from the melt (unrelaxed models).

Honeycutt−Andersen bond-pair analysis, we assume that two atoms within the cutoff radius R_o = 1.245 are neighbors, where the cutoff distance is the position of the minimum after the first peak in the radial distribution function (RDF) for the amorphous state obtained at T = 0.3 (see Figure 1). Final amorphous configurations were well-relaxed before calculating static quantities. In order to improve the statistics, we average the results over two independent runs. In addition, in order to test the stability of an amorphous structure, we have relaxed amorphous models obtained at T = 0.8 and T = 1.0 by relaxation at zero pressure for 1.093 μs if taking Ar for testing, and their amorphous structure remains unchanged after such relatively long annealing. Note that the crystallization pattern and the limit of the liquid's thermodynamic stability under cooling of a monatomic simple 2D system with the same LJG potential have been discussed clearly in ref 14, and we do not address these issues again here. That is, an amorphous state has been obtained at several cooling rates, and glass transition temperature is shown to be an increasing function of the cooling rate.[14] It was found that in a relatively high-temperature region, amorphous state gradually transforms into crystals and the time−temperature−transformation curve shows a typical nose shape. The transformation time to a crystalline state is the shortest at temperature 14−15% below the melting temperature and at the sufficiently low temperatures the system does not transform into a crystalline state within a long simulation time studied, indicating the long-lived glassy state of the system (see ref 14).

III. EVOLUTION OF STRUCTURE AND STABILITY OF GLASSY STATE

Evolution of structure on cooling from the melt can be observed through temperature dependence of the radial distribution function and bond−pairs of Honeycutt−Andersen analysis. Figure 1 shows RDF at various temperatures. At high temperatures, RDF shows a shape typical of normal liquids. When the temperature is reduced, the height of peaks in RDF is enhanced and splitting of the second peak in RDF appears like that commonly found in metallic glasses of close-packed metals. To get more detailed information on local order in the system upon cooling from the melt, we analyzed the temperature dependence of various bond-pairs obtained by Honeycutt−Andersen analysis, which is shown in Figure 2. In Honeycutt−Andersen analysis,[5,13] the structure is analyzed by pairs of atoms on which

dx.doi.org/10.1021/jp111086e |J. Phys. Chem. B XXXX, XXX, 000–000

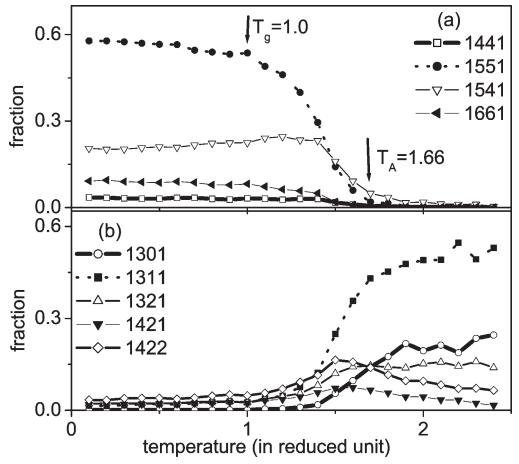

Figure 2. Temperature dependence of different bond-pairs in the system upon cooling from the melt (unrelaxed models).

four indices are assigned: (i) the first index indicates whether or not they are near neighbors and is 1 if the pair is bonded and 2 otherwise, where we used the fixed cutoff radius R_o = 1.245 for determining the nearest-neighbor pairs as described before; (ii) the second index is equal to the number of near neighbors they have in common; (iii) the third index is equal to the number of bonds among common near neighbors; and (iv) the fourth index denotes existence of the structure with the same first three indices but with different arrangement.

In the high temperature region ($T > T_A$) we found the existence of various bond-pairs of non-close-packed atomic arrangement typical for the normal simple monatomic liquids such as 1301 and 1311 (see ref 5) (Figure 2b). Their dominated fractions are almost temperature independent in this high temperature region, which indicates the homogeneous structure of the normal liquid state. When the temperature is reduced below T_A, their fraction steeply decreases. In contrast, the fraction of the bond-pairs of close-packed atomic arrangement typical for supercooled liquids and glasses such as 1541, 1551, 1441, and 1661 is very small in the high temperature region ($T > T_A$), and below T_A their fraction increases with further decreasing temperature (Figure 2a). The largest increment was found for the 1551 bond-pair in that it progressively grows up in the supercooled region ($T_g < T < T_A$), reaching a saturation-dominated value for the glassy state of around 0.56−0.57 (for unrelaxed configurations). Note that finding almost the same fraction of 1551 bond-pair for an amorphous Fe model[23] and increment of fraction of the 1551 pair indicates an enhancement of icosahedral local order in the system, since the 1551 pair is direct evidence of local 5-fold symmetry. Local isocahedral order has been also found in our models like that found in simple supercooled liquids and glasses.[5,10,15,23] The fraction of 1541 is the second largest in the glassy state (Figure 2a). Although the 1541 cluster has five neighbors, these five neighbors have only four bonds. Therefore, the 1541 cluster can be considered to have a distorted 5-fold symmetrical structure, and Voronoi statistics based on the number of faces cannot distinguish a difference between 1551 and 1541 pairs. Such a 1541 bond-pair is related to the defective icosahedra and it is also commonly found in glasses.[5,10,23] This means that the energy-favored local structure of the LJG glass is the icosahedral order, which is incompatible with the global crystallographic symmetry. Arrest of the increase

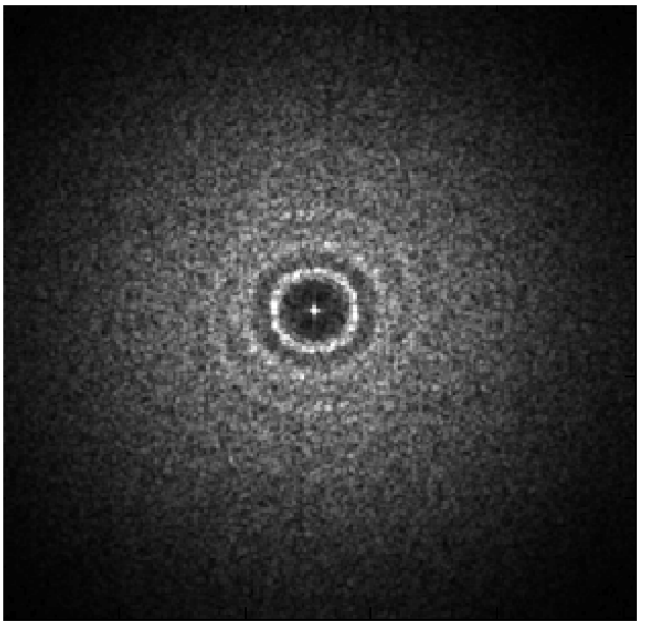

Figure 3. Static diffraction image on the k_z = 0 plane of glassy state at T = 0.8 obtained after annealing for 6.18 ns if taking Ar for testing.

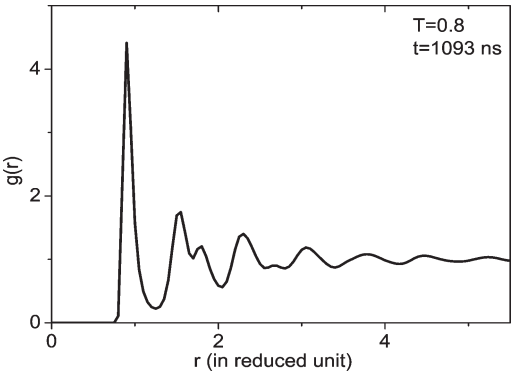

Figure 4. RDF of the glassy state at T = 0.8 obtained after 1093 ns annealing if taking Ar for testing.

of various bond-pairs of close-packed atomic arrangement including 1551 pairs at T_g = 1.0 is a signature of a glass transition at this point. This is the origin of long-lived stability of LJG glass since 5-fold symmetry frustrates the crystallization. We show in Figure 3 the static structure factor on the k_z = 0 plane of the system at T = 0.8. This is similar to that observed experimentally for the bulk metallic glasses[24] and thus we can see clearly the glassy nature of the system.

In order to check the stability of glassy state obtained at low temperatures, we annealed models obtained at T = 1.0 and 0.8 for a long annealing of 1093 ns and confirmed that their glassy state remains unchanged. Note that glass of the monatomic system with LJ interatomic potential easily crystallizes after annealing for 0.045−0.300 ns (see refs 8 and 9). Our results indicate that the monatomic glass with LJG interatomic potential is indeed a long-lived one. The RDF of the model at T = 0.8 obtained after 1093 ns annealing is shown in Figure 4. One can see that it is almost the same as that obtained for unrelaxed models presented in Figure 1. We also show static structure factor, $S(Q)$, of the

dx.doi.org/10.1021/jp111086e |J. Phys. Chem. B XXXX, XXX, 000–000

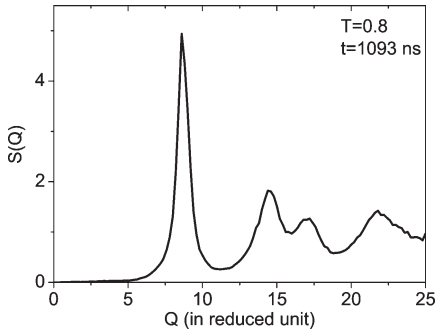

Figure 5. Structure factor, $S(Q)$, of the glassy state at $T = 0.8$ obtained after 1093 ns annealing if taking Ar for testing; the amplitude of wave vector Q is in unit of σ^{-1}.

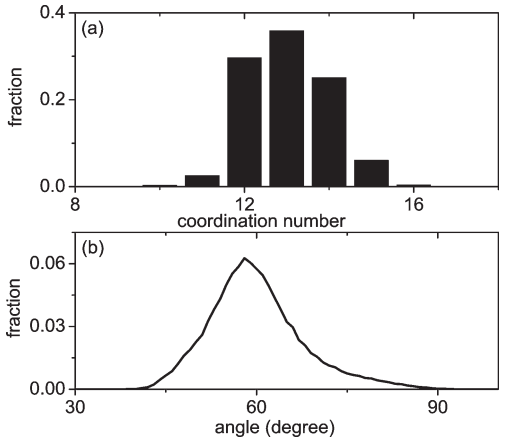

Figure 6. Coordination number distribution (a) and bond-angle distribution (b) of the glassy state at $T = 0.8$ obtained after 1093 ns annealing if taking Ar for testing.

model at $T = 0.8$ obtained after 1093 ns annealing (Figure 5). One can see clear splitting of the second peak in $S(Q)$, which is related to the existence of icosahedral order in the system. More detailed information about the local structure in the system can be found via coordination number and bond-angle distributions shown in Figure 6. We found that more than 95% of atoms in the models have a coordination number from 12 to 15. The broad coordination number distribution indicates an inhomogeneous structure of the system. About 30% of atoms have 12 nearest neighbors, which might be related to the standard icosahedrons (13 atoms including atom at the center). The majority of atoms in the system has 13 nearest neighbors that are related to the defective icosahedra (i.e., a polyhedron consisting of some 1551, 1661, and/or 1441 bonds). On the other hand, there is a significant amount of atoms that have coordination number $Z = 14$ and 15. These structural units might be related to the Frank−Kasper polyhedra.[25] Moreover, bond-angle distribution has a single peak at around 60°, which indicates the domination of equilateral triangles in the system, which is related to the faces of icosahedra or Frank−Kasper polyhedra.[25] Almost the same coordination number and bond-angle distributions have been found for amorphous Fe models.[23] Note that mean coordination number for the amorphous state of our LJG model is $Z = 13.03$ and almost the same value was obtained for an amorphous Fe model.[23] This confirms our suggestion that monatomic glass with LJG interatomic potential can primarily include a glassy state of close-packed metals.

Table 1. Relative Fraction of Bond-Pairs in Relaxed Models of LJG Models Obtained at $T = 1.0$ after Different Aging Times

aging time (ns)	1301	1311	1321	1421	1422	1441	1551	1541	1661
6.18	0.002	0.023	0.023	0.024	0.042	0.028	0.556	0.220	0.082
618	0	0.008	0.011	0.009	0.016	0.027	0.664	0.167	0.098
1093	0	0.009	0.009	0.010	0.017	0.024	0.665	0.169	0.096

Annealing time dependence of various bond-pairs in the model obtained at $T = 1.0$ is listed in Table 1. One can see that after long annealing, the fraction of 1551 pair increases from about 0.56 to 0.66 and the system reaches a stable glassy state; i.e., fraction of various bond-pairs is almost unchanged after 618 ns of annealing. The fraction of the 1551 pair in the stable glassy state is very high, around 0.66−0.67. This means that annealing significantly enhances the local icosahedral order in the system. A very high fraction of the 1551 pair in the annealed system is the origin of the long-lived stability of the glassy state of the system, since the 5-fold symmetry of the 1551 pair frustrates the crystallization. In addition, there is no tendency of crystallization of the system during annealing, since the fraction of the bond-pairs related to the crystalline orders such as 1441 and 1661 (bond-pairs are characteristic of bcc crystalline structure) or 1421 and 1422 (bond-pairs which are characteristic of fcc and hcp crystalline structures) remains very small and unchanged even after long annealing (Table 1).

IV. THERMODYNAMIC AND DYNAMIC PROPERTIES

Via the temperature dependence of potential energy per atom in the system, important characteristic temperatures, such as glass transition temperature ($T_g = 1.0$) and crossover temperature ($T_A = 1.66$), of the system have been found.[26] That is, the temperature dependence of this quantity shows clearly three characteristic regions. The linear part in the high-temperature region is related to the equilibrium liquid state. Consequently, the point of the start of deviation from linearity, $T_A = 1.66$, can be considered as a crossover temperature to other state. This point is also related to the change in diffusion mechanisms of atoms from the liquid-like into solid-like dynamics; i.e., the inverse temperature dependence of the logarithm of the diffusion constant changes slope at this point.[26] Similarly, the linear part of the lowest temperature region of the curve is related to the glassy state. The point of the start of deviation from linearity, $T_g = 1.0$, can be considered as a glass transition temperature. These linear parts are separated by the intermediate region, i.e., that of $T_g < T < T_A$ (see ref 26). The temperature dependence of mass density obtained in the present work also shows similar trends; i.e., the density of the system increases with decreasing temperature, and critical points (i.e., T_A or T_g) can be also determined via deviation from the linearity of high- or low-temperature parts of the curve (Figure 7). This ensures that evolution of the structure and thermodynamics in the system on cooling from the melt is accompanied by the changes in atomic packing in the system.

As shown in Figure 7, mass density increases with decreasing temperature. Therefore, atomic arrangement becomes more close-packed with decreasing temperature; especially mass density strongly increases for the region $T_g < T < T_A$, reaching the

dx.doi.org/10.1021/jp111086e |J. Phys. Chem. B XXXX, XXX, 000–000

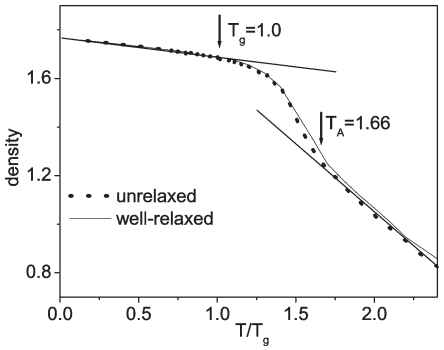

Figure 7. Temperature dependence of mass density of the system upon cooling from the melt (straight lines serve as guide for eyes).

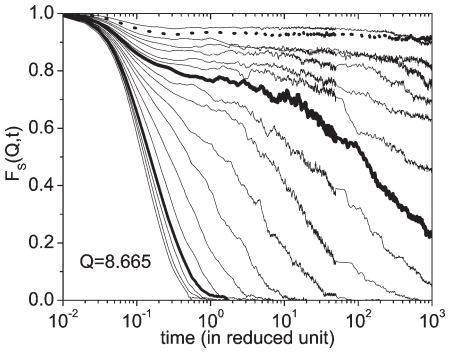

Figure 8. Time dependence of the incoherent intermediate scattering function for temperatures ranging from $T = 2.0$ to 0.3 (from left to right). The curves for models obtained at $T = 1.7$ (i.e., close to $T_A = 1.66$), $T_g = 1.0$, and $T_f = 0.4$ are presented in the green, bold, and dotted lines, respectively. The amplitude of wave vector $Q = 8.665\sigma^{-1}$ is the location of the first peak in the structure factor, $S(Q)$. The curves for the deeply supercooled region are relatively noisy compared with those obtained in the high-temperature region, which may be related to the heterogeneous behavior of the dynamics of atoms in this region.

saturated value for glassy state of around $\rho = 1.70$ at T_g. Increasing of mass density (or increasing of the degree of atomic packing) enhances a trapped-diffusive motion of atoms, and below a certain temperature all atoms become trapped and nontrapped motion cannot occur again as stated in ref 27. Indeed, we found the same scenario for diffusion of atoms in LJG liquids; i.e., at T_A the inverse temperature dependence of logarithm of diffusion constant changes slope into the dramatically slowing down diffusion regime. Namely, T_A can be considered as a crossover temperature between liquid-type and solid-type dynamics[27] or crossover temperature T_C predicted by the mode-coupling theory (MCT) as well.[28] Note that we have the ratio $T_A/T_g = 1.66$ in the present work and it is slightly higher than $T_A/T_g \sim 1.30$ for various glass-forming materials suggested by Angell.[29] It is clear that the dramatic decrease of the diffusion on cooling occurs within a narrow temperature interval below a crossover temperature (T_A) and eventually results in total structural arrest at the glass transition point (T_g). The dramatic slowing down of liquid dynamics on cooling toward the glassy state was thought to be related to the appearance of CRRs in the supercooled region;[18] we will highlight the situation in the subsequent sections.

In passing, the evolution of various bond-pairs observed on cooling of the system from the melt toward glassy state is consistent with the temperature dependence of potential energy, mass density, and diffusion constant. This indicates strong correlations between them in the vitrification process. In particular, the change in atomic mechanism of diffusion at T_A is indeed related to the corresponding change in atomic arrangement in the system, i.e., the change from non-close-packed to more close-packed at the same point (Figure 2). Strong enhancement of the close-packed atomic arrangement in the range $T_g < T < T_A$, which is consistent with the progressive increase of the mass density for the same temperature range (Figure 7), stimulates the activated diffusion process.

In order to investigate the dynamic behavior of the system in more detail, we computed $F_S(Q,t)$, the incoherent intermediate scattering function for the wave vector with amplitude $Q = 8.665\sigma^{-1}$ which is the location of the first peak in structure factor, $S(Q)$. The function $F_S(Q,t)$ measures essentially the dynamics of a tagged particle within its cage and how it escapes this cage at long times, the function form is given below

$$F_S(Q,t) = \frac{1}{N}\sum_{j=1}^{N}\langle \exp\{iQ[r_j(t) - r_j(0)]\}\rangle \qquad (2)$$

where $r_j(t)$ is the location of particle j at time t and Q is a wave-vector. One can see in Figure 8 that $F_S(Q,t)$ has the ballistic motion of particles at short times, and at high temperatures, the curves show at very short time a crossover from ballistic regime to a relaxation behavior that is basically exponential and that the correlation function decays to zero within one τ_0 (i.e., reduced time unit; see Figure 8), i.e., very rapidly. For intermediate and low temperatures, we observe additional behaviors: (i) immediately after the ballistic regime, which lasts just up to around $0.1-0.2\tau_0$, the motion of the particle enters to a plateau regime, the strength and length of which increase rapidly with decreasing temperatures, and at $T \leq T_f$ ($T_f = 0.4$) the plateau regime lasts for infinity; (ii) the nonexponential behavior of the curves at longer time occurs after a plateau regime for temperatures of $1.6 > T > T_f$. Similar behaviors of the time dependence of $F_S(Q,t)$ have been found for various glass-forming supercooled liquids.[19,30] The plateau regime is related to the caging effects, i.e., the temporary trapping of the particles by their neighbors. The time window in which the correlator is close to the plateau is the "β-relaxation time", and the time window in which the correlator falls below the plateau is the "α-relaxation time". First, one can see in Figure 8 that at $T > T_A$ (i.e., at $T \geq 1.7$) the dynamics of the particle in the equilibrium liquid state exhibits homogeneous behavior, and the curves of $F_S(Q,t)$ are very similar each to other; i.e., they show at very short times a crossover from ballistic regime to a relaxation behavior that is basically exponential and the correlation function decays to zero within one unit of time (τ_0). At temperatures below T_A, the curves start to deviate from those of higher temperatures: the plateau regime occurs, which is enhanced with decreasing temperatures, and the long time part of the curves changes from an exponential behavior to a non-exponential one. At $T \leq 1.0$, the plateau regime is clearly shown and it is long-lasting. This indicates the strong caging effects of a glassy state. This means that the glass transition temperature is indeed $T_g = 1.0$, like that observed above via corresponding changes in thermodynamic quantities. At $T \leq T_f$ ($T_f = 0.4$), after the ballistic regime at very short times the function $F_S(Q,t)$ remained in the plateau regime for an infinity of time at a very large value of around 0.93−0.95. This indicates the occurrence of full solidification (complete glass

dx.doi.org/10.1021/jp111086e |J. Phys. Chem. B XXXX, XXX, 000–000

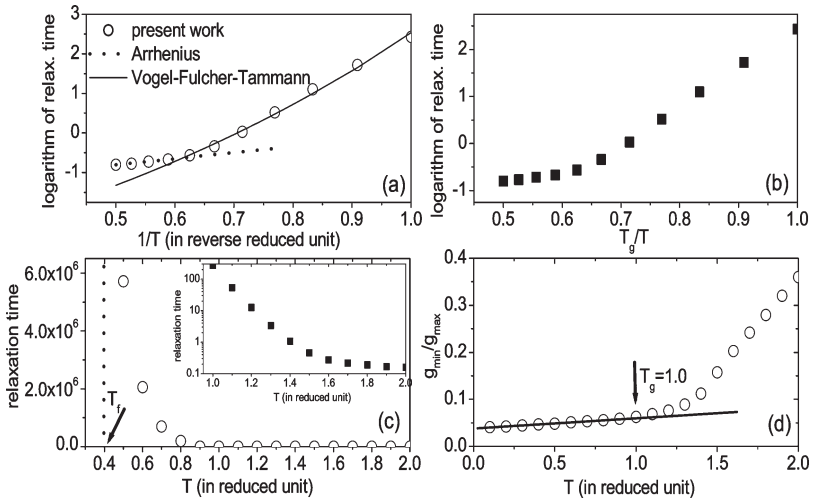

Figure 9. (a) Inverse temperature dependence of the logarithm of α-relaxation time, i.e., log τ_α vs $1/T$. (b) T_g-scaled Arrhenius plot of α-relaxation time. (c) Temperature dependence of α-relaxation time; the inset shows part of the curve for $1.0 \leq T \leq 2.0$. (d) Temperature dependence of the Wendt−Abraham ratio of the system upon cooling from the equilibrium liquid to the glassy state.

Table 2. Parameters Obtained by Fitting the Temperature Dependence of $\tau_\alpha(T)$ to Arrhenius $[\tau_\alpha(T) = \tau'_{\alpha 0} \exp(A/T)]$ and Vogel−Fulcher−Tammann $[\tau_\alpha(T) = \tau_{\alpha 0} \exp[B/(T - T_{VFT})]]$ Laws[a]

$\tau'_{\alpha 0}$	A	$\tau_{\alpha 0}$	B	T_{VFT}
2.6057×10^{-2}	3.5851 ± 0.2052	2.3061×10^{-4}	8.5272 ± 0.2663	0.40

[a] All parameters are in corresponding reduced units.

formation) in the system at $T_f = 0.4$ (we will discuss about this phenomenon below).

One of the most universal properties of supercooled liquids and glasses is the relaxation behavior, which differs from that observed in less viscous liquids. Approaching the glass transition, their average α-relaxation time, $\tau_\alpha(T)$, shows non-Arrhenius thermal activation, and in many cases the temperature dependence of $\tau_\alpha(T)$ can be described by the empirical Vogel−Fulcher−Tammann (VFT) equation

$$\tau_\alpha(T) = \tau_{\alpha 0} \exp[B/(T - T_{VFT})] \quad (3)$$

where $\tau_{\alpha 0}$, B, and T_{VFT} are parameters. Equation 3 becomes the Arrhenius law if we set $T_{VFT} = 0$; T_{VFT} is the so-called Vogel−Fulcher−Tammann temperature, the temperature at which $\tau_\alpha(T)$ would diverge to infinity. We defined $\tau_\alpha(T)$ as the time required for the correlation function to decay to e^{-1} of its initial value [i.e., as the intersection point of the horizontal line of $F_S(Q,t) = e^{-1}$ and corresponding curves presented in Figure 8]. Note that we can find $\tau_\alpha(T)$ for our system by this way just at temperatures $T \geq T_g$; at temperatures below T_g it is impossible due to the strong caging effects of the glassy state. In the present work, at $T < T_g$ we found $\tau_\alpha(T)$ via extrapolation to longer times. Data obtained for $\tau_\alpha(T)$ are shown in Figure 9.

The plot of log τ_α vs $1/T$ (open circles in Figure 9a) exhibits clearly a non-Arrhenius behavior. Note that none of the commonly used phenomenological laws describes the variation of the log τ_α over the entire experimental temperature range. The dotted line in Figure 9a shows that the Arrhenius law is followed only for the high-temperature range ($T \geq 1.7$), which corresponds to the dynamics in an equilibrium liquid state. The solid line in Figure 9a indicates that VFT law is followed well for the lower temperature region, i.e., for $1.6 \geq T \geq T_g$. A similar tendency was found for the temperature dependence of α-relaxation time in the simple glass-forming liquid *m*-toluidine.[31] Parameters of these laws are shown in Table 2. On the other hand, the nonlinearity of the T_g-scaled Arrhenius plot of α-relaxation time (Figure 9b) presents the fragility of the system with LJG potential used in simulations, the fragility index m of the system can be defined via the slope of the curve at $T = T_g$, i.e., $m = [\partial(\log \tau_\alpha(T))/\partial(T_g/T)]_{T=T_g}$. In addition, the temperature dependence of the α-relaxation time is shown in Figure 9c, and one can see that $\tau_\alpha(T)$ remained almost constant at a small value (small fraction of reduced time unit τ_0) in the high-temperature region (at $T \geq 1.7$) of equilibrium liquid state. It increases upon further decreasing the temperature and reaches a large value of $\tau_\alpha(T_g) = 269.5\tau_0$ at the glass transition (see the inset in Figure 9c). However, $\tau_\alpha(T)$ dramatically grows with further cooling below the glass transition and it has an extremely large value (see Figure 9c) that is impossible to determine from MD simulations [we found $\tau_\alpha(T)$ for $T < T_g$ by extrapolation]. The quantity $\tau_\alpha(T)$ indeed diverges at $T = T_f$. This confirms again the validity of the VFT law as described above and $T_f = 0.4$ in our model is equal to the Vogel−Fulcher−Tamman temperature (T_{VFT}). It is clear that due to the simplicity of the model used in the present simulation, relaxation time τ_α at the glass transition is underestimated compared with that found in practice. However, the temperature dependence of τ_α qualitatively agrees with that commonly found in practice (see ref 31 and references therein).

We also show the temperature dependence of the Wendt−Abraham ratio[32] (i.e., g_{min}/g_{max}, where g_{min} and g_{max} are the magnitudes of the first minimum and first maximum of the RDF) of the system upon cooling from the equilibrium liquid to the glassy state (Figure 9d). The point of starting from the linearity of the curve of the low-temperature region at $T = 1.0$ can be

dx.doi.org/10.1021/jp111086e |J. Phys. Chem. B XXXX, XXX, 000–000

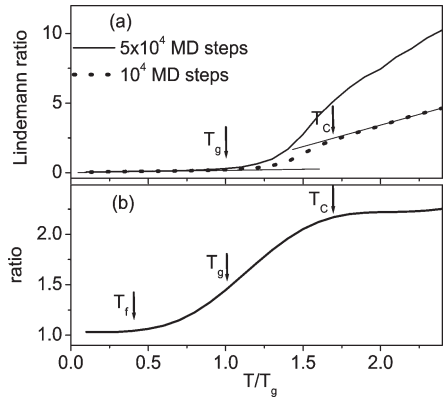

Figure 10. (a) Temperature dependence of the Lindemann ratio (δ_L) of atoms in models (straight lines serve as guide for eyes). (b) Temperature dependence of the ratio $\delta_L(5\tau_C)/\delta_L(\tau_C)$.

considered the glass transition temperature. This confirms again that $T_g = 1.0$ found above via analyzing various thermodynamic properties is correct.

V. ATOMIC MECHANISM OF VITRIFICATION PROCESS

Lindemann Criterion. In order to elucidate the atomic mechanism of the vitrification process, we classify atoms into two groups by their fluidity. We first obtain the mean squared displacement (MSD) of atom i, i.e., $\langle \Delta r_i^2 \rangle$, during a characteristic time, τ_C, which is chosen appropriately. Then, we define the kind of Lindemann ratio of the atom by $\delta_i = \langle \Delta r_i^2 \rangle^{1/2}/\overline{R}$, where the mean interatomic distance $\overline{R} = 0.9$ is equal to the position of the first peak in the RDF of a glassy state. From the analysis of the MSD of atoms, we found that $\tau_C = 10\tau_0$ is an adequate choice (i.e., 10^4 MD steps of relaxation or 24.4 ps), which corresponds to the end of plateau regime of MSD.[26] We set the demarcation value to $\delta_C = 0.21$ (see below), that is atoms with $\delta_i \leq \delta_C$ are classified as solid-like and atoms with $\delta_i > \delta_C$ are classified as liquid-like. More detail about different methods of defining solid-like or liquid-like atoms in supercooled liquids can be seen in ref 26.

We define the Lindemann ratio δ_L of the system by the average of δ_i over all atoms, $\delta_L = \Sigma_i \delta_i/N$. The temperature dependence of the Lindemann ratio is shown in Figure 10. It is interesting to note that the Lindemann ratio and the potential energy[26] show similar temperature dependence, indicating a strong correlation between them in the vitrification process. Critical points such as $T_A = 1.66$ (or $T_C = 1.66$) and $T_g = 1.0$ can be found again here from the deviation of the linearity in high- and low-temperature dependence of δ_L. Hence, we can find the critical value for δ_L in Figure 10 and at $T = T_g$ it is equal to 0.21. This means that the critical value for the Lindemann ratio is $\delta_C = 0.21$ and the corresponding critical value of MSD of atoms is $\langle \Delta r_C^2 \rangle = 0.035$ (in reduced unit). Therefore, atoms with $\delta_i \leq 0.21$ can be considered as solid-like ones. Note that for bcc crystals $\delta_C = 0.18$ (ref 22), for Lennard-Jones fcc crystal $\delta_C = 0.22$ (ref 33). To the best of our knowledge, this is the first time a full temperature dependence of the Lindemann ratio was obtained for a large temperature range which covers equilibrium liquid, supercooled liquid, and glassy regions. Our MD simulation data presented in Figure 10 do not support the speculation about the temperature dependence of δ_L proposed in ref 22. Moreover, no suggestion had been made in ref 22 for the glassy state. For the supercooled liquid region, they proposed just a straightforward extension from the data for equilibrium liquid.[22] Figure 10 shows that δ_L in the simple monatomic system decreases with decreasing temperature, and it can be separated into three distinct parts: (i) the first linear part reflects the high-temperature region (for equilibrium liquid state, i.e., at $T > T_C$); (ii) the progressive decrease of δ_L on further cooling is related to the region of $T_g < T < T_C$ and it clearly deviates from the linear part of the high-temperature dependence for equilibrium liquids; and (iii) the second linear part of the curve is related to the glassy state in lower temperature region, for which δ_L is very small and it is mainly related to the vibrations of atoms around their equilibrium positions in the solid state (at $T \leq T_g$). One point here, the temperature region of $T_g < T < T_C$, should include the supercooled region ($T_g < T < T_m$) and the narrow region of higher temperature ($T_m < T < T_C$), where T_m is the melting point of the system, which is located not very far below T_C. We have no data for T_m since the crystalline state of the present 3D system cannot be obtained even using a much lower cooling rate (not shown). We can infer indirectly T_m (see below).

It should be emphasized that δ_L depends on the demarcation time τ_C. In order to highlight the situation, we compared the Lindeman ratio determined for 5 times longer demarcation time of $5\tau_C$ (or 5×10^4 MD steps). We plot the ratio $\delta_L(5\tau_C)/\delta_L(\tau_C)$ against temperature in Figure 10b. We can see clearly four regimes as follows. For $T \leq T_f$, the ratio is unity, indicating that atoms do not move out from their localized position. When the temperature is in the range $T_f \leq T \leq T_g$, the ratio becomes slightly larger than unity, which is the evidence that liquid-like atoms appear. When the temperature is increased from the glass transition temperature to the crossover one ($T_g < T < T_C$), the ratio increases rapidly. In the normal liquid state above the crossover temperature ($T \geq T_C$), the ratio increases moderately again. We found that the ratio $\delta_L(5\tau_C)/\delta_L(\tau_C) = 5^{1/2}$ and 1.0 at $T = T_C$ and $T = T_f$, respectively (see Figure 10b). Consequently, in this way we can identify clearly these characteristic temperatures.

Note that the curves, similar to that for δ_L presented in Figure 10a, were found for the temperature dependence of the symmetry coefficients of local clusters in supercooled Fe models.[34] They denoted the upper transition temperature (equivalent to T_A in the present work) as T_{g2}, at which percolation of icosahedral clusters is attained, while at $T_g < T_{g2}$ the aggregation of icosahedral clusters is arrested.[34] We also found that although an increase of icosahedral order is indeed arrested at T_g (see Figure 2a), the fraction of local icosahedral order in our system is too small at around T_A (or T_{g2} in ref 34) and that no percolation of icosahedral clusters was found around this point (Figure 2a).

Behavior of Solid-like Atoms in Supercooled and Glassy States. Since the occurrence and clustering of solid-like atoms during vitrification process in the system have been clearly presented in ref 26, we just briefly describe the phenomenon here. Concerning glass formation, we emphasize here previously unreported data as follows: (i) the interplay between solid-like and liquid-like atoms during vitrification, (ii) the annealing time dependence of the fraction of solid-like atoms in the system at a given temperature, and (iii) the behavior of liquid-like atoms in supercooled and glassy states. We detected solid-like atoms by the Lindemann criterion $\delta_i \leq \delta_C$ with $\tau_C = 10\tau_0$, and we found that solid-like atoms occur in the region a bit below T_C. That is, the first 15−16 solid-like atoms appear throughout the model at $T/T_g = 1.5$, and the fraction of solid-like atoms ($p = n_S/N$)

dx.doi.org/10.1021/jp111086e |J. Phys. Chem. B XXXX, XXX, 000–000

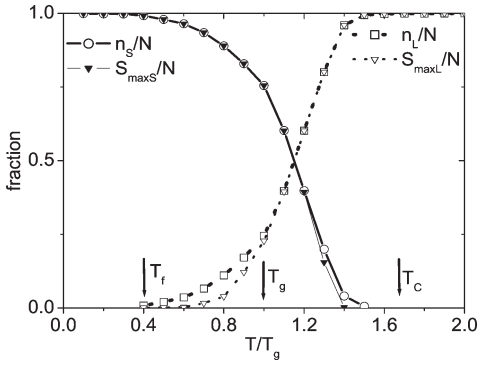

Figure 11. Fraction of solid-like and liquid-like atoms (n_S/N and n_L/N) and the ratio of the size of the largest cluster of solid-like and liquid-like atoms to the total number of atoms in the system ($S_{max\,S}/N$ and $S_{max\,L}/N$) as a function of temperature.

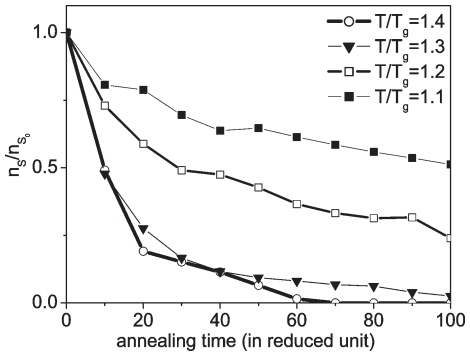

Figure 12. Annealing time dependence of the fraction of solid-like atoms in models obtained at different temperatures (n_S is a number of solid-like atoms at the annealing time t_a compared with the initial one, i.e n_{S0}).

increases with decreasing temperature, as shown by the thin and thick solid curves in Figure 11. The increment is small in the first stage of the supercooled region and then it progressively increases, reaching about 0.75 at the glass transition and 1.00 at $T/T_g < 0.40$. This means that full solidification of the system occurs at $T = T_f = 0.40$. It is clear that the first solid-like atoms occur at $T = 1.5$ below $T_C = 1.66$. Temperature $T = 1.5$ can be considered as the melting point (T_m) of the system, since we have $T_m/T_g = 3/2$, like that commonly found for glass-forming systems.[19] This means that the region $1.0 < T/T_g < 1.5$ is a supercooled one of the system.

Solid-like atoms have a tendency to form clusters even in the initial stage of their formation; we regard that two atoms are connected in one cluster when their distance is less than the radius of the first coordination sphere, i.e., $R_o = 1.245$. Upon further cooling, much larger clusters appear and the largest cluster progressively grows up (Figure 11; see more detail in ref 26). Subsequently, a single percolation cluster occurs and the number of solid-like atoms aggregated in this percolation cluster sharply increases on further cooling to form a glassy phase. A single percolation cluster was formed via merging of small-size coarse clusters and single solid-like atoms when the fraction of solid-like atoms reaches the critical value $p_C = 0.40$ at $T/T_g = 1.20$. This percolation cluster spans throughout the model (the curves for n_S/N and $S_{max\,S}/N$ begin to coincide at $T/T_g = 1.20$; see Figure 11). The value $p_C = 0.40$ lies within the range $0.15 \leq p_C \leq 0.45$ suggested in ref 35. It was suggested that the last infinite cluster of solid-like atoms disappear at T_C (ref 36). However, our calculations show that such a point must be located at a temperature much lower than T_C, since the first solid-like atoms occur only at $T/T_g = 1.50$, which is located below $T_C = 1.66$. On the other hand, Figure 11 also pointed out that full solidification occurs at $T_f = 0.40$, which is identical to the Vogel–Fulcher–Tammann[37] (T_{VFT}) or Kauzmann temperature.[38] We found that $T_C/T_g = 2 - T_f/T_g$ (ref 26).

One can see that the occurrence and growing length scale of solid-like clusters in supercooled liquid region accompany the corresponding occurrence and growth of icosahedral local order in the same temperature region (see the curve for the 1551 pair in Figure 2a). This ensures that in simple monatomic systems with LJG interatomic potential, the noncrystallographic energy-favored local configurations are found to be icosahedral ones. Local icosahedral configurations form extended domains the size of which grows as the temperature decreases toward T_g, like that found for the system with Dzugutov's one.[39] As discussed above, it was found that solid-like atoms form clusters in the early stage of the supercooled region, and it is the origin of the structural and dynamical heterogeneities in supercooled liquids in general.[18,40] This is consistent with the earlier observation associating low mobility domains in supercooled liquids with lower energy and a higher degree of local ordering.[17,41]

We investigated the lifetime of solid-like clusters by annealing the system for a longer time at constant temperature. Namely, we first classified solid-like atoms with τ_C and obtained the number of solid-like atoms n_{S0}, and then we restarted the MD simulation for time t_a and recalculated the MSD including this additional time, i.e., for $\tau_C + t_a$. From this new MSD, we obtained δ_i for atom i and judged if it is still solid-like or not. We then obtained the number of solid-like atoms as a function of the annealing time t_a. Dependence of the ratio $n_S(t_a)/n_{S0}$ on the annealing time is shown in Figure 12. From Figure 12, we can see that the lifetime of solid-like clusters is rather long and the clusters were totally melted after annealing for about $60\tau_0$ and $100\tau_0$ (or 6×10^4 and 10^5 MD steps) at temperatures $T/T_g = 1.40$ and 1.30, respectively. These times correspond to 146.4 and 244 ps if we use parameters of Ar, which are much longer than the typical lifetime 1 ps of icosahedral cluster in liquid Fe model obtained at 1900 K (ref 34). However, in the deeply supercooled region such as $T/T_g = 1.20$ and 1.10, total melting of a single percolation solid-like cluster was not found for the long annealing time studied; i.e., the size of the percolation solid-like cluster was only reduced to about 16% and 54% of the initial one after annealing for $200\tau_0$ (or 2×10^5 MD steps), respectively (not shown in Figure 12). This means that the lower the temperature is, the larger the size of solid-like clusters and the longer their lifetime. In addition, due to the relatively low stability (compared with those of percolation solid-like clusters at lower temperatures) of solid-like clusters obtained at $T/T_g = 1.40$ and 1.30, the number of solid-like atoms monotonically decreases with annealing time. The nonmonotonic behavior seen at $T/T_g = 1.20$ and 1.10 is due to the fluctuation in cluster formation (Figure 12).

Behavior of Liquid-like Atoms in Supercooled and Glassy States. We also investigated the evolution of liquid-like atoms in the system as a function of temperature, which is shown as the dotted and dashed curves in Figure 11. One can see that the number of liquid-like atoms is a constant maximal value at $T > T_C$, which is expected for the equilibrium liquid region. Then, it decreases with decreasing temperature and vanishes at

dx.doi.org/10.1021/jp111086e |J. Phys. Chem. B XXXX, XXX, 000–000

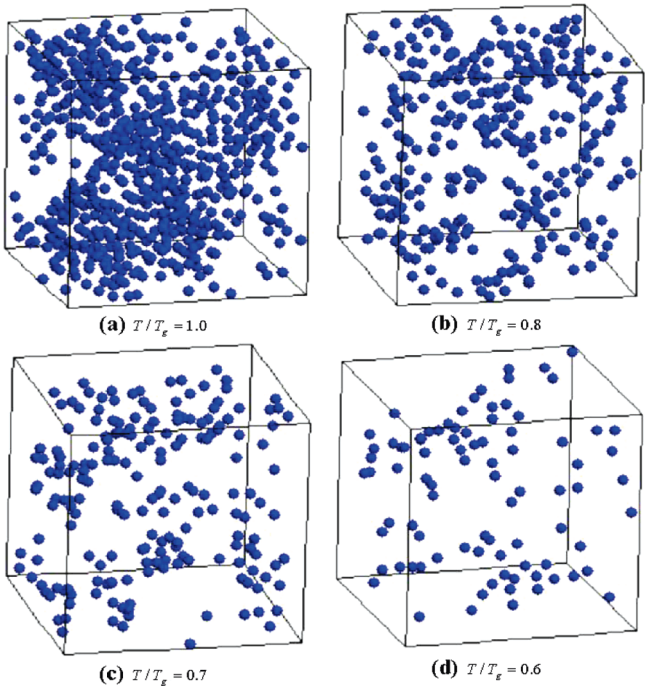

Figure 13. 3D visualization of the collective appearance of the liquid-like atoms in glassy models obtained at $T \leq T_g$.

around $T/T_g = 0.4$ (i.e., at $T = T_f = 0.40$) when full solidification occurs in the system. Liquid-like atoms also have a tendency to form clusters, and the size of the percolation cluster is also constant for the region $T > T_C$. It decreases with decreasing temperature as expected (see the curve for $S_{max\,L}/N$ in Figure 11). Subsequently, the percolation liquid-like cluster disappears at around $T/T_g = 1.1$ when liquid-like atoms become the minority in the system, and after that it splits into several smaller liquid-like clusters in the glassy matrix at temperatures below T_g. The threshold for disappearance of percolation liquid-like cluster is around the critical concentration of liquid-like atoms $p_C = 0.40$, which is the same as the percolation threshold of solid-like atoms obtained in the previous section. This means that a percolating liquid-like cluster can exist only for $T > T_g$. Therefore, the phenomenological speculation stated in ref 36, i.e., a percolating liquid-like cluster exists at $T < T_g$, is not correct.

It is interesting to note that liquid-like atoms exist even below the glass transition (Figure 13). A significant amount of liquid-like atoms in the glassy state can play an important role in the stability and various thermodynamic properties of glasses. We found that their percentage is about 25%, 17.5%, 11.2%, and 6.8% at $T/T_g = 1.0$, 0.9, 0.8, and 0.7, respectively. At $T/T_g = 1.0$, they are found throughout the glassy matrix, although they are strongly correlated (see Figure 13a). Below T_g, the glassy system becomes relatively rigid, and therefore, liquid-like atoms contained within the glassy matrix are thermally arrested. Indeed, even after a long annealing of 2×10^5 MD steps we found that MSD of atoms (including liquid-like ones) at $T < T_g$ is rather small; i.e., the MSD remains smaller than the critical value for determining solid-like atoms (not shown). On the other hand, the atomic displacement distribution (ADD) for liquid-like atoms at $T < T_g$ shows that their atomic mobility is very slow (see Figure 14). That is, while ADD in normal liquid (at $T/T_g = 2.0$) has a typical Gaussian form distributed over a large range of

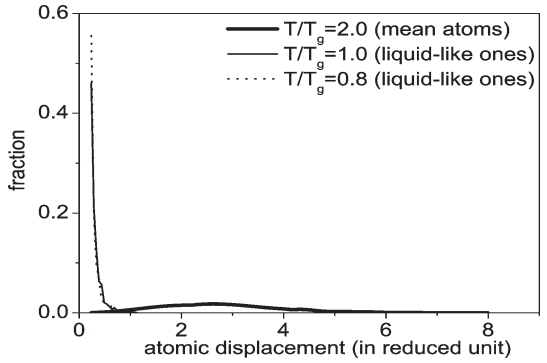

Figure 14. Atomic displacement distribution of liquid-like atoms in models obtained at $T/T_g = 1.0$ and 0.8 compared with that for the normal liquid at $T/T_g = 2.0$ after the same relaxation time of $10\tau_0$.

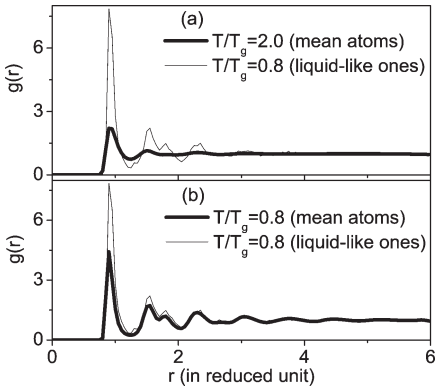

Figure 15. Radial distribution function of liquid-like atoms in the model obtained at $T/T_g = 0.8$ compared with that of the mean atoms in models obtained at $T/T_g = 2.0$ and $T/T_g = 0.8$.

atomic displacements, the main fraction of liquid-like atoms at $T \leq T_g$ has very small atomic displacement, which just slightly exceeds a critical value for determining solid-like atoms (Figure 14). This means that due to dense packing of liquid-like atoms and their distribution in frozen glassy matrix, liquid-like atoms in this region exhibit a behavior quite different from that of their counterparts in the normal liquid state.

Indeed, the RDF and ADD show that liquid-like atoms in the glassy state exhibit "strongly arrested" behavior rather than a liquid-like one, since their RDF is typical for the glassy state (Figure 15a) and their ADD is quite different from that of the normal liquid. Moreover, the existence of liquid-like atoms below T_g is the origin of significant diffusion in the corresponding temperature region (not shown). That is, the MSD of atoms at $T = 0.7$ has a tendency to grow up after relaxation of about 3×10^4 MD steps, indicating the existence of significant diffusion (not shown). However, diffusion quickly decreases at lower temperatures and it vanishes at around $T_f = 0.40$, i.e., the MSD of atoms at temperatures $T \leq T_f$ remained constant for a long annealing time (not shown). On the other hand, liquid-like atoms are strongly correlated, and therefore, local liquid-like clusters may act as local sources of destabilization of the glassy state. It may lead to the crystallization of corresponding glasses in general. Note that crystallization of the glassy state of a 2D system with the same LJG interatomic potential has been found recently.[14] On the other hand, strongly correlated liquid-like

dx.doi.org/10.1021/jp111086e |J. Phys. Chem. B XXXX, XXX, 000–000

atoms existing below T_g are the origin of atomic dynamics or dynamical heterogeneities below the glass transition, which were found by MD simulations,[30,42−44] and our simulations highlight the situation (see Figure 15b). Liquid-like atoms contained in a large cluster of solid-like atoms can move within the area by exchanging their positions without causing diffusive motion or structural relaxation for most of the times. This dynamic is the origin of the Johari−Goldstein process.[45] In this situation, atoms can move only in a concerted manner, which gives rise to the dynamical heterogeneity.[42−44] Occasionally, those atoms can experience structural relaxation when other solid-like atoms cooperate. The area causing the structural relaxation can be considered as the cooperatively rearranging region (CRR) proposed by Adam and Gibbs.[46] The size of the CRR increases as the fraction of the solid-like atoms increases.

VI. CONCLUSIONS

We have presented comprehensive MD simulations for simple monatomic system with LJG interatomic potential in three dimensions and we found clear evidence of long-lived glass formation. We investigated the atomic mechanism of the vitrification process on the basis of the temperature dependence of various properties, including the potential energy, diffusion, and spatiotemporal arrangement of solid-like and liquid-like atoms (these atoms are distinguished by the Lindemann parameter). Several conclusions can be made here as follows:

(i) We found that the glass of a monatomic liquid with LJG interatomic potential contains a large fraction of local icosahedral order (up to 66−67% of total orders existed in well-relaxed system) due to competing of two nearest-neighbor distances of double-well interaction. Local icosahedral structure is the origin of the stability of the glassy state of the monatomic LJG system, and indeed, crystallization of our 3D glassy system has not been found for very long annealing up to 1.093 μs. Note that crystallization of 2D glass with the same LJG interatomic was found by MD simulations after very long annealing.[14] It seems that much longer annealing time is needed in order to observe crystallization of our 3D glassy system.

(ii) A crossover from liquid-like to solid-like dynamics on cooling the system from a high temperature melt into a supercooled region found in ref 26 is consistent with the temperature dependence of mass density, the Lindemann ratio, and bond-pairs in the present work. In addition, the temperature dependence of the Lindemann ratio for a wide temperature range does not support the speculations proposed in literature.

(iii) We found the temperature dependence of incoherent intermediate scattering function, $F_S(Q,t)$, and α-relaxation time, $\tau_\alpha(T)$, of the system for a wide temperature range from the equilibrium liquid to deep glassy states. The time−temperature dependence of $F_S(Q,t)$ shows clearly that the system is a glass former. We found that the temperature dependence of $\tau_\alpha(T)$ follows the Vogel−Fulcher−Tammann law for the temperature region close to T_g and it diverges to infinity at $T = 0.4$, which is located much below the glass transition temperature. At higher temperatures (in the equilibrium liquid state) $\tau_\alpha(T)$ follows the Arrhenius law.

(iv) Serious corrections for the phenomenological speculations in different scenarios of the glass transition can be made on the basis of our MD simulations. First, the statement that the glass transition occurs at the percolation threshold of solid-like clusters in supercooled liquids[35,41,47,48] is not correct. The glass transition is indeed related to the percolation process of solid-like atoms in the system; however, it occurs not at the percolation threshold of solid-like clusters but at significantly lower temperature, where the majority of atoms in the system is solid-like to form a relatively rigid solid phase. It was suggested that there are two percolation thresholds related to the glass formation.[36] That is, the first percolation cluster of liquid-like atoms appears at T_1, the last percolation cluster of solid-like atoms disappears at T_2, and $T_1 < T_g < T_2$ (ref 36). They argued that T_1 and T_2 are close to the Vogel−Fulcher−Tammann and MCT critical temperatures, respectively. This understanding is not correct either. Our calculations pointed out that the first percolation liquid-like cluster can exist only at $T > T_g$ and no percolation threshold at around T_C was found.

(v) The atomic mechanism of glass formation described in the present work is fully consistent with the free energy landscape picture of the glass transition proposed in ref 49, since the appearance of solid-like clusters must be reflected in the structure of the free energy landscape. That is, larger clusters indicate that deep basins are formed in the free energy landscape and that the structural relaxation becomes slower. In particular, we found that the characteristic temperatures of glass formation satisfy the characteristic temperature relation predicted by the trapping diffusion model.[27] The trapping diffusion model is a simplified expression of the free energy landscape theory of the glass transition.[49]

(vi) Note that we also found the same atomic mechanism of glass formation in supercooled Fe liquid models with the Pak−Doyam interactomic pair potential (our unpublished data), which is a single well interaction potential (see ref 23 and references therein). This means that results of the present work could be applicable to systems with other interatomic potentials.

(vii) We found a significant amount of strongly correlated liquid-like atoms in glassy models obtained below the glass transition. Although they exhibit "strong thermally arrested" behavior rather than liquid-like one due to very slow mobility and close atomic packing between them (i.e., they are thermally arrested within the solid glassy matrix), they may act as the local sources of destabilization of the glassy state. It may lead to the crystallization of glasses. Moreover, they are the origin of local atomic dynamics like the Johari−Goldstein process in glasses[45] or dynamics and dynamical heterogeneities below the glass transition.[30,42−44]

AUTHOR INFORMATION

Corresponding Author

*E-mail: vvhoang2002@yahoo.com.

ACKNOWLEDGMENT

We would like to thank Dr. Michael Engel of Stuttgart University for providing us the computer program of the structure analysis. V.V.H. thanks the Vietnam National Foundation

for Science and Technology Development for the financial support under Grant Number 103.02.12.09. The work at Tokyo Denki University was partially supported by JSPS KAKENHI Grant-in-Aid for Scientific Research (C) 19540405 and 225-40400 and Research Institute for Science and Technology of Tokyo Denki University Grant Number Q10G-01.

REFERENCES

(1) Donth, E. *The Glass Transition: Relaxation Dynamics in Liquids and Disordered Materials*; Springer-Verlag: Berlin, 2001.
(2) Rahman, A.; Mandell, M.; McTague, J. *J. Chem. Phys.* **1976**, *64*, 1564.
(3) Steinhardt, P. J.; Nelson, D. R.; Ronchetti, M. *Phys. Rev. B* **1983**, *28*, 784.
(4) Nose, S.; Yonezawa, F. *J. Chem. Phys.* **1986**, *84*, 1803.
(5) Honeycutt, J. D.; Andersen, H. C. *J. Phys. Chem.* **1987**, *91*, 4950.
(6) Shneidman, V. A.; Uhlmann, D. R. *J. Non-Cryst. Solids* **1998**, *224*, 86.
(7) Robles, M.; de Haro, M. L. *EuroPhys. Lett.* **2003**, *62*, 56.
(8) Nishio, K.; Koga, J.; Yamaguchi, T.; Yonezawa, F. *J. Phys. Soc. Jpn.* **2004**, *73*, 627.
(9) Hoang, V. V. *Physica B* **2010**, *405*, 1908.
(10) Dzugutov, M. *Phys. Rev. A* **1992**, *46*, R2984.
(11) Dzugutov, M. *Phys. Rev. Lett.* **1993**, *70*, 2924.
(12) Engel, M.; Trebin, H.-R. *Phys. Rev. Lett.* **2007**, *98*, 225505.
(13) Hoang, V. V.; Odagaki, T. *Physica B* **2008**, *403*, 3910.
(14) Mizuguchi, T.; Odagaki, T. *Phys. Rev. E* **2009**, *79*, 051501.
(15) Evteev, A. V.; Kosilov, A. T.; Levchenko, E. V. *J. Exp. Theor. Phys.* **2004**, *99*, 522.
(16) Dzugutov, M.; Simdyankin, S. I.; Zetterling, F. H. M. *Phys. Rev. Lett.* **2002**, *89*, 195701.
(17) Donati, C.; Glotzer, S.; Poole, P.; Kob, W.; Plimpton, S. *Phys. Rev. E* **1999**, *60*, 3107.
(18) Ediger, M. D. *Annu. Rev. Phys. Chem.* **2000**, *51*, 99.
(19) Debenedetti, P. G.; Stillinger, F. H. *Nature (London)* **2001**, *410*, 259.
(20) Stevenson, J. D.; Schmalian, J.; Wolynes, P. G. *Nat. Phys.* **2006**, *2*, 268.
(21) Lindemann, F. A. *Z. Phys.* **1910**, *11*, 609.
(22) Stillinger, F. H. *Science* **1995**, *267*, 1935.
(23) Hoang, V. V.; Cuong, N. H. *Physica B* **2009**, *404*, 340.
(24) Miller, M.; Liaw, P., Eds. *Bulk Metallic Glasses*; Springer: New York, 2007.
(25) Qi, D. W.; Wang, S. *Phys. Rev B* **1991**, *44*, 884.
(26) Hoang, V. V.; Odagaki, T. *Solid State Commun.* **2010**, *150*, 1971.
(27) Odagaki, T. *Phys. Rev. Lett.* **1995**, *75*, 3701.
(28) Goetze, W. In *Liquids, Freezing and the Glass Transition*; Hansen, J. P., Levesque, D., Zinn-Justin, J.; Eds.; Elsevier: Amsterdam, 1991.
(29) Angell, C. A. *J. Phys. Chem. Solids* **1988**, *49*, 863.
(30) Kob, W. *J. Phys.: Condens. Matter* **1999**, *11*, R85.
(31) Cuttroni, M.; Mandanici, A. *J. Chem. Phys.* **2001**, *114*, 7118.
(32) Wendt, H. R.; Abraham, F. F. *Phys. Rev. Lett.* **1978**, *41*, 1244.
(33) Jin, J. H.; Gumbsch, P.; Lu, K.; Ma, E. *Phys. Rev. Lett.* **2001**, *87*, 055703.
(34) Tomida, T.; Egami, T. *Phys. Rev. B* **1995**, *52*, 3290.
(35) Cohen, M. H.; Grest, G. S. *Phys. Rev. B* **1979**, *20*, 1077.
(36) Novikov, V. N.; Rossler, E.; Malinovsky, V. K.; Surovtsev, N. V. *Europhys. Lett.* **1996**, *35*, 289.
(37) Vogel, H. *Phys. Z.* **1921**, *22*, 645. Fulcher, G. S. *J. Am. Ceram. Soc.* **1925**, *8*, 339.
(38) Kauzmann, W. *Chem. Rev.* **1948**, *43*, 219.
(39) Zetterling, F. H. M.; Dzugutov, M.; Simdyankin, S. I. *J. Non-Cryst. Solids* **2001**, *293*−*295*, 39.
(40) Ediger, M. D.; Angell, C. A.; Nagel, S. R. *J. Phys. Chem.* **1996**, *100*, 13200.
(41) Egami, T.; Tomida, T.; Kulp, D.; Vitek, V. *J. Non-Cryst. Solids* **1993**, *156*−*158*, 63.
(42) Vollmayr-Lee, K.; Kob, W.; Binder, K.; Zippelius, A. *J. Chem. Phys.* **2002**, *116*, 5158.
(43) Vollmayr-Lee, K. *J. Chem. Phys.* **2004**, *121*, 4781.
(44) Vollmayr-Lee, K.; Zippelius, A. *Phys. Rev. E* **2005**, *72*, 041507.
(45) Johari, J. P.; Goldstein, M. *J. Chem. Phys.* **1971**, *55*, 4245.
(46) Adams, G.; Gibbs, G. H. *J. Chem. Phys.* **1965**, *43*, 139.
(47) Turnbull, D.; Cohen, M. H. *J. Chem. Phys.* **1958**, *29*, 1049. Grest, G. S.; Cohen, M. H. *Adv. Chem. Phys.* **1981**, *48*, 454.
(48) Cyrot, M. *J. Phys. (Paris)* **1980**, *41*, C8–107.
(49) Odagaki, T.; Yoshimori, A. *J. Non-Cryst. Solids* **2009**, *355*, 681.